

(1)–2.729 (9) Å. In none of these other cases are the pairs of adjacent polar coordination sites bridged by a bidentate ligand. Nevertheless, the Nb=Nb distance found here, 2.711 (3) Å, is about in the middle of the previously established range. Far from being shorter than any of the others, it is third from the shortest. Thus, while the presence of a pair of bridging $R_2PCH_2PR_2$ ligands can sometimes have a dramatic effect on the M–M distance (as illustrated by the comparison of $Re_2Cl_6(dppe)_2$, which has chelating diphosphine ligands and $Re\cdots Re = 3.809$ (1) Å,¹⁶ and

$Re_2Cl_6(dppm)_2$, which has bridging diphosphine ligands and $Re-Re = 2.616$ (1) Å³), this factor is not of major importance in these doubly bonded systems formed by the trivalent group 5 metals niobium and tantalum.

Acknowledgment. We are grateful to the National Science Foundation and the Robert A. Welch Foundation (Grant No. A-494) for support.

Registry No. 1, 98858-56-1; 2, 98858-57-2; $[V_2Cl_3(THF)_6]_2[Zn_2Cl_6]$, 89172-48-5; $Nb_2Cl_6(THT)_3$, 98858-58-3; Nb, 7440-03-1.

Supplementary Material Available: Tables of observed and calculated structure factors and anisotropic displacement parameters for both compounds, a full listing of bond angles for 1, and listings of selected least-squares planes for 2 and torsional angles for $Nb_2Cl_6(dmppm)_2$ and $M_2Cl_6(dppm)_2$, M = Mo, Re (15 pages). Ordering information is given on any current masthead page.

- (16) Jaecker, J. A.; Robinson, W. R.; Walton, R. A. *J. Chem. Soc., Dalton Trans.* 1975, 698.
 (17) In this paper the periodic group notation is in accord with recent actions by IUPAC and ACS nomenclature committees. A and B notation is eliminated because of wide confusion. Groups IA and IIA become groups 1 and 2. The d-transition elements comprise groups 3 through 12, and the p-block elements comprise groups 13 through 18. (Note that the former Roman number designation is preserved in the last digit of the new numbering: e.g., III → 3 and 13.)

Contribution from the Department of Chemistry,
 The University of North Carolina at Chapel Hill, Chapel Hill, North Carolina 27514

Ferromagnetic Intramolecular Interactions in a Bis(μ -bromo)-Bridged Copper(II) Dimeric Compound: Crystal Structure and Molecular Structure Determination, Electron Paramagnetic Resonance Studies, and Magnetic Susceptibility Measurements on Bis(μ -bromo)bis[(diethylenetriamine)copper(II)] Perchlorate

DEBRA K. TOWLE,¹ S. K. HOFFMANN,² WILLIAM E. HATFIELD,*¹ PHIRTU SINGH,¹ PHALGUNI CHAUDHURI,³ and KARL WIEGHARDT³

Received April 16, 1985

The compound bis(μ -bromo)bis[(diethylenetriamine)copper(II)] perchlorate, $[Cu_4H_{13}N_3Br]_2(ClO_4)_2$, crystallizes in the monoclinic space group $C2/c$ (C_{2h}^2 , No. 15) with unit cell dimensions $a = 23.054$ (8) Å, $b = 7.669$ (1) Å, $c = 14.061$ (9) Å, and $\beta = 116.02$ (3)°. There are four dimers in the unit cell. The structure consists of parallel planar bis(μ -bromo)-bridged copper(II) dimers and essentially uncoordinated perchlorate anions. The geometry at each copper(II) is distorted tetragonal pyramidal with the basal ligands being three nitrogens from the diethylenetriamine ligand and one bromine, and the apical position is occupied by an inversion-related bromine atom. The dimeric unit is axial-equatorial in nature. The bridging bromide ligands are axial to one copper and equatorial to the other. The copper–bromide bond lengths are 2.424 (1) Å (equatorial) and 2.887 (1) Å (apical), and the Cu–Br–Cu' angle is 90.63°. Analysis of temperature-dependent magnetic susceptibility data shows that the compound is ferromagnetic with a singlet–triplet splitting (ΔE_{ST}) of +2.7 cm⁻¹. EPR spectra of a powdered sample were collected at room temperature and at 77 K. EPR spectra of single crystals exhibit a strong merging effect between lines from magnetically nonequivalent dimers in the unit cell. Neither fine structure nor hyperfine structure was resolved down to 77 K. Molecular g factors of individual copper(II) ions were determined from angular dependence measurements on single crystals in a coplanar three-axial reference system to be $g_z = 2.208$ (1), $g_y = 2.055$ (1), and $g_x = 2.052$ (1). The line widths of the EPR lines display atypical angular dependence, i.e. $\Delta B_{pp}(\theta)$ does not reflect $g^2(\theta)$. This unusual behavior is explained in terms of an unresolved zero-field splitting resulting from intradimer dipolar coupling.

Introduction

The structural and magnetic properties of bis(μ -hydroxo) and bis(μ -chloro)-bridged complexes have been intensively studied.^{4–10} Copper(II) ions in most of the bis(μ -chloro) bimetallic complexes are antiferromagnetically exchange coupled with small singlet–triplet (ΔE_{ST}) splittings,^{7–9} although examples of triplet ground state, ferromagnetically coupled systems are known.⁸ The singlet–triplet splittings in many of these chemically and structurally related compounds exhibit a strong correlation with the structural

parameter ϕ/R , where ϕ is the Cu–Cl–Cu bridge angle and R is the longer bridge bond distance.

There is less information available about the structural and magnetic properties of bis(μ -bromo)-bridged copper(II) dimers. A correlation between the magnetic and structural characteristics of these complexes has yet to be found.

The compound formulated as $Cu(dien)Br(ClO_4)$ (dien = diethylenetriamine) contains bis(μ -bromo)-bridged dimers in which the copper(II) ions are ferromagnetically exchange coupled. Here we describe the results of synthetic, structural, magnetic, and EPR studies on $[Cu_2(dien)_2Br_2](ClO_4)_2$.

Experimental Section

Synthesis. Diethylenetriamine, 1.1 mL (10 mmol), was added with constant stirring to a solution of 2.23 g (10 mmol) of $CuBr_2$ in 40 mL of water. Solid $NaClO_4$ (approximately 2.5 g) was added to this deep blue solution. The solution was filtered to remove any solid particles. The filtrate was left at room temperature until deep blue crystals formed (2 days). The crystals were collected by filtration, washed with ethanol and ether, and air dried. Anal. Calcd for $Cu_2(C_4H_{13}N_3)_2Br_2(ClO_4)_2$: C, 13.88; H, 3.79; N, 12.14. Found: C, 14.03; H, 3.84; N, 12.01.

X-ray Data Collection. A blue crystal of the compound was mounted at the end of a glass fiber attached to a goniometer head and was used throughout the X-ray work. The cell constants were obtained by a least-squares refinement of the setting angles of 25 reflections. The

- (1) The University of North Carolina at Chapel Hill.
 (2) Permanent address: Institute of Molecular Physics, Polish Academy of Sciences, 60-179 Poznan, Poland.
 (3) Ruhr-Universität Bochum, Bochum, West Germany.
 (4) Crawford, V. H.; Richardson, H. W.; Wasson, J. R.; Hodgson, D. J.; Hatfield, W. E. *Inorg. Chem.* 1976, 15, 2107.
 (5) Hatfield, W. E. *ACS Symp. Ser.* 1974, No. 5, 108.
 (6) Hodgson, D. J. *Prog. Inorg. Chem.* 1975, 19, 173.
 (7) Roundhill, S. G. N.; Roundhill, D. M.; Bloomquist, D. R.; Landee, C.; Willett, R. D.; Dooley, D. M.; Gray, H. B. *Inorg. Chem.* 1979, 18, 831.
 (8) Marsh, W. E.; Patel, K. C.; Hatfield, W. E.; Hodgson, D. J. *Inorg. Chem.* 1983, 22, 511.
 (9) Marsh, W. E. Ph.D. Dissertation, The University of North Carolina at Chapel Hill, 1982.
 (10) Hatfield, W. E. *Comments Inorg. Chem.* 1981, 1, 105.

Table I. Crystal Data for $[\text{Cu}(\text{dien})\text{Br}]\text{ClO}_4$

fw ($\text{CuBrC}_4\text{H}_{13}\text{N}_3\text{ClO}_4$)	346.1
space group	C_{2h}^2-c2/c (No. 15)
a , Å	23.054 (8)
b , Å	7.669 (1)
c , Å	14.061 (9)
β , deg	116.02 (3)
V , Å ³	2233.8
Z	8
d_{calcd} , g cm ⁻³	2.06
$\mu(\text{Mo K}\alpha)$, cm ⁻¹	57.5
cryst size, mm	0.60 × 0.50 × 0.30
diffractometer	CAD-4
radiation	Mo K α ($\lambda_\alpha = 0.7107$ Å)
scan method	graphite monochromator
data collec limit, deg	$\omega-2\theta$
no. of unique data collected	$2 \leq 2\theta \leq 54$
no. of data used, $F_o \geq 3\sigma(F_o)^2$	2624
no. of variables	1686
R	127
R_w	0.051
	0.055

Table II. Positional Parameters of the Non-Hydrogen Atoms and Their Estimated Standard Deviations^a

atom	x	y	z
Br	0.27502 (3)	0.3721 (1)	0.12745 (5)
Cu	0.18484 (4)	0.1755 (1)	0.03858 (6)
Cl	0.10080 (9)	0.3014 (3)	0.2239 (1)
O(1)	0.1447 (3)	0.239 (1)	0.1900 (4)
O(2)	0.1324 (3)	0.349 (1)	0.3308 (4)
O(3)	0.0680 (4)	0.149 (2)	0.2282 (8)
O(4)	0.0617 (6)	0.410 (2)	0.1551 (7)
N(1)	0.2263 (3)	-0.0320 (9)	0.1300 (4)
N(2)	0.1102 (2)	0.0093 (9)	-0.0378 (4)
N(3)	0.1219 (3)	0.3676 (9)	-0.0331 (5)
C(1)	0.1874 (4)	-0.186 (1)	0.0834 (6)
C(2)	0.1164 (4)	-0.135 (1)	0.0337 (6)
C(3)	0.0504 (3)	0.115 (1)	-0.0736 (6)
C(4)	0.0610 (4)	0.284 (1)	-0.1172 (6)

^a In parentheses.

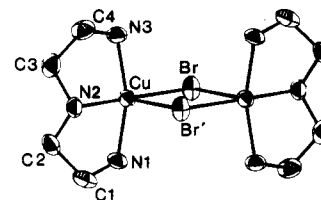
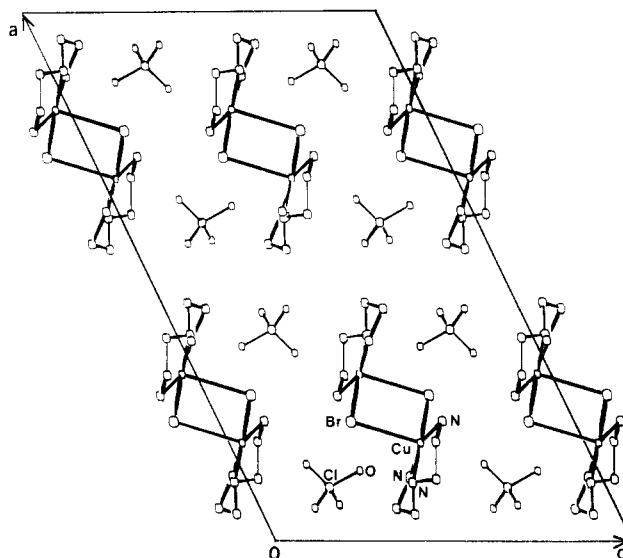
intensity data were collected by the $\omega-2\theta$ scan technique, the scan range in ω being $1.0 + 0.35 \tan \theta$ with a 25% extension at either end of a peak for background measurement. All data were measured at 20 ± 2 °C. Pertinent experimental conditions and crystallographic data are summarized in Table I.

Data were corrected for background and Lorentz and polarization effects. An empirical absorption correction based on the average variation in intensity in an azimuthal scan of nine reflections with χ near 90° was applied. The transmission factor ranged from 0.465 to 1.000. The scattering factors were corrected for anomalous dispersion effects. The systematic absences in the intensity data were consistent with the space groups Cc or $C2/c$. The latter space group was assumed and later confirmed by the successful refinement of the structure.

Structure Determination and Refinement. The bromine and copper atoms were located from a three-dimensional Patterson synthesis and the remaining non-hydrogen atoms from a difference Fourier synthesis. Refinement was carried out with use of anisotropic thermal parameters for all the non-hydrogen atoms. The hydrogen atoms attached to carbons were placed in calculated positions with a C-H distance of 1.0 Å and an isotropic temperature factor B of 5.0. The function minimized was $\sum w(|F_o| - |F_c|)^2$. The weighting factor, w , was taken as $4F_o^2/\sigma^2(F_o)^2$, where $\sigma^2(F_o)^2$ is the variance of F_o^2 and is derived from counting statistics. The positional parameters derived from the last cycle of refinement are given in Table II. The thermal parameters and the observed and calculated structure amplitudes are available as supplementary material.

All calculations were performed on a PDP-11 computer using the Structure Determination Package provided by the Enraf-Nonius Corp. Drawings were made with use of ORTEP-II.¹¹

Magnetic Susceptibility Measurements. Magnetic susceptibility data were collected on a powdered sample by using a PAR Model 155 vi-

**Figure 1.** View of the $[\text{Cu}_2(\text{dien})_2\text{Br}_2]^{2+}$ cation. The thermal ellipsoids are drawn at the 40% probability level. Hydrogen atoms are omitted.**Figure 2.** Projection of the crystal structure of $[\text{Cu}_2(\text{dien})_2\text{Br}_2](\text{ClO}_4)_2$ along the b axis. One unit cell is outlined.**Table III.** Bond Distances (Å) in the Cation $[\text{Cu}(\text{dien})\text{Br}]^+$

Cu-Cu' ^a	3.790 (1)	N(1)-C(1)	1.452 (7)
Cu-Br	2.424 (1)	C(1)-C(2)	1.522 (7)
Cu-Br'	2.887 (1)	N(2)-C(2)	1.460 (6)
Cu-N(1)	2.005 (4)	N(2)-C(3)	1.484 (6)
Cu-N(2)	2.029 (4)	C(3)-C(4)	1.499 (8)
Cu-N(3)	2.003 (4)	N(3)-C(4)	1.525 (6)

^a The primed atoms are related to the corresponding unprimed atoms through a center of inversion.

brating-sample magnetometer equipped with a Janis Research Co. liquid-helium Dewar and operated at 10 KG. The magnetometer was calibrated with $\text{HgCo}(\text{NCS})_4$.¹² A calibrated GaAs diode was used to monitor the sample temperature. The data were corrected to compensate for the diamagnetism of the constituent atoms and for the temperature-independent paramagnetism of the Cu(II) ions (60×10^{-6} cgsu).¹³⁻¹⁶

EPR Spectra. EPR spectra were recorded at X-band on a Varian E-109 spectrometer with a rectangular TE₁₀₂ cavity. The magnetic field was calibrated with a DPPH marker, and the frequency was monitored with a Hewlett-Packard 5245L frequency counter. Powder spectra were obtained at room and liquid-nitrogen temperatures. The angular dependence of the single-crystal spectra was recorded in an arbitrary orthogonal reference system, 1, 2, 3, with axis 3 perpendicular to the cleavage plane of the crystal and axis 1 along the longest crystal edge in this plane.

Results

Description of the Structure. The molecular structure of $[\text{Cu}_2(\text{dien})_2\text{Br}_2]^{2+}$ is shown in Figure 1. The Cu(II) ion has 4

(11) Johnson, C. K. *Oak Ridge Natl. Lab., [Resp.] ORNL (U.S.) 1976, ORNL-5138.*

- (12) Brown, D. B.; Crawford, V. H.; Hall, J. W.; Hatfield, W. E. *Inorg. Chem.* **1977**, *16*, 1303.
 (13) McKim, F. R.; Wolf, W. P. *J. Sci. Instrum.* **1957**, *34*, 64.
 (14) Figgis, B. N.; Lewis, J. In "Modern Coordination Chemistry"; Lewis, J., Wilkins, R. G., Eds.; Interscience: New York, 1960; Chapter 6, p 403.
 (15) König, E. "Magnetic Properties of Transition Metal Compounds"; Springer-Verlag: West Berlin, 1966; Landolt-Börnstein Series.
 (16) Weller, R. R.; Hatfield, W. E. *J. Chem. Educ.* **1979**, *56*, 652.

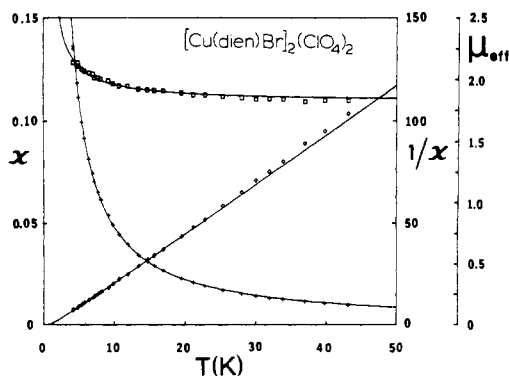


Figure 3. Plot of the molar magnetic susceptibility, χ (cgsu), the inverse susceptibility, $1/\chi$, and the effective magnetic moment, μ_{eff} , as a function of temperature for a powdered sample of $[\text{Cu}_2(\text{dien})_2\text{Br}_2](\text{ClO}_4)_2$. The solid lines represent the best least-squares fit of eq 1b to the data with the parameters given in the text.

+ 1 coordination with the three nitrogens of the diethylenetriamine ligand and the bromine atom forming the basal plane of a distorted square pyramid. A bromine atom from a centrosymmetrically related cation occupies the apical site of the pyramid. The copper-copper separation of 3.790 Å (Table III) is consistent with a dimer formulation for the complex. The Cu-Br-Cu' bridging angle is 90.63°, and the Br-Cu-Br' angle is 89.37°. The two Br atoms and the two Cu atoms of the dimer are exactly planar, there being a center of inversion in the middle of the dimer. The dimeric cations and the perchlorate anions are packed in alternate rows running parallel to the *a* axis of the crystal axis as shown in Figure 2.

Magnetism. The molar magnetic susceptibility, inverse susceptibility, and effective magnetic moment of the complex are plotted as a function of temperature in Figure 3. The intradimer exchange Hamiltonian is of the form $-2J\hat{S}_1\cdot\hat{S}_2$, from which $-2J = \Delta E_{\text{ST}}$ for a pair of $S = 1/2$ ions, the magnetic susceptibility expression, can be derived.¹⁷ In the case of $[\text{Cu}_2(\text{dien})_2\text{Br}_2](\text{ClO}_4)_2$, the magnetic susceptibility expression for two exchange-coupled $S = 1/2$ ions, eq 1a, with a molecular field correction resulting in eq 1b,¹⁸ was used.

$$\chi_m = \frac{Ng^2\beta^2}{3kT} [1 + \frac{1}{3} \exp(-2J/kT)]^{-1} \quad (1a)$$

$$\chi_{\text{cor}} = \frac{\chi_m}{1 - [2zJ'\chi_m/Ng^2\beta^2]} \quad (1b)$$

The solid lines in Figure 3 represent the result obtained from fitting eq 1b to the data by using a Simplex fitting routine¹⁹ with the EPR-determined *g* value of 2.104 as a constant parameter. The best fit was found with $2J = +2.7 \text{ cm}^{-1}$ and $zJ' = 0.83 \text{ cm}^{-1}$.

The solid lines in Figure 3 correspond to the data very well. In the low-temperature region the molar magnetic susceptibility and μ_{eff} increase rapidly with decreasing temperature. This may be explained as being due to pretransitional effects arising from the onset of a low-temperature transition to three-dimensional ferromagnetic ordering in the crystal or to the presence of an impurity. Inclusion of a percent-impurity parameter in the fitting routine neither improved the fit to the data nor changed the value of $2J$ appreciably.

EPR Powder Spectra. The EPR spectra of a powdered sample of $[\text{Cu}(\text{dien})\text{Br}]\text{ClO}_4$ at 295 and 77 K are shown in Figure 4, where rather featureless spectra may be seen. Although there is some change in the line shape, there is no increase of resolution with temperature change.

Single-Crystal EPR Spectra. Single crystals suitable for EPR measurements were obtained by very slow crystal growth from

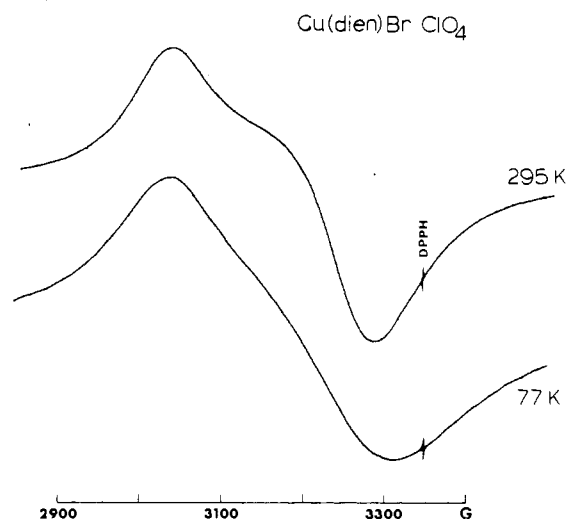


Figure 4. EPR X-band powder spectra of $[\text{Cu}_2(\text{dien})_2\text{Br}_2](\text{ClO}_4)_2$ at room temperature and 77 K.

aqueous solution. The EPR spectrum of a single crystal contains one line in all crystal orientations. Hyperfine splitting and zero-field splitting fine structure were not observed in the spectra in any crystal orientation. Hyperfine structure is generally not resolved in EPR spectra of magnetically condensed copper(II) compounds.

The fine-structure splitting in exchange-coupled bimetallic copper(II) compounds is expected to have two contributions: (1) an anisotropic exchange contribution as a result of spin-orbit coupling and (2) a contribution from magnetic dipolar coupling between Cu(II) ions. Anisotropic exchange contributions have their maximum values along the *z* axis of an individual copper(II) ion and are given by the expression^{20,21}

$$D_z^{\text{ex}} = -(g_z - 2)^2 J_1 / 48 \quad (2)$$

where the ground state of the Cu(II) ion is $d_{x^2-y^2}$ and J_1 is an exchange integral between the ground state $d_{x^2-y^2}$ of one copper(II) ion in a dimer and an excited d_{xy} state of the second ion. This exchange is expected to be ferromagnetic and generally much larger than exchange $2J$ between ground states of the copper(II) ions as has been proved for a series of bis(μ -hydroxo)-bridged copper(II) complexes²¹ and also observed in heterodinuclear complexes.²²

Even if we can assume $J_1 = 35 \text{ cm}^{-1}$ in $[\text{Cu}_2(\text{dien})_2\text{Br}_2](\text{ClO}_4)_2$, i.e. more than 10 times larger than $2J$, the anisotropic exchange contribution, from eq 2, to the total **D** tensor will be on the order of 0.0315 cm^{-1} (about 320 G). The contribution to the total **D** tensor from the intradimer dipolar splitting is expected to be maximal along the Cu-Cu direction. This dipolar contribution to the **D** tensor can be estimated as $D^{\text{dip}} (\text{cm}^{-1}) = 0.433g_z^2/r^3$, where *r* (in Å) is the Cu-Cu separation. In $[\text{Cu}_2(\text{dien})_2\text{Br}_2](\text{ClO}_4)_2$ $r = 3.79 \text{ Å}$ and $D^{\text{dip}} = 0.0388 \text{ cm}^{-1}$ (about 390 G). Thus, D^{dip} is about twice as large as that expected for hyperfine splitting from the copper ions. In spite of the quite larger values of D^{ex} and D^{dip} , zero-field splitting is not resolved in the EPR spectra. This observation indicates that the zero-field splitting must be dynamically averaged as a result of mobile excitations in the crystal.

The line shapes are Lorentzian, and the line width varies from 50 to 105 G at room temperature. Since there are four dimers in the unit cell, it is clear that the resonance lines have merged as a result of an exchange interaction. An EPR spectrum with merging lines can be described in terms of stochastic theory²³⁻²⁵

(17) Bleaney, B.; Bowers, K. D. *Proc. R. Soc. London, Ser. A* **1952**, *214*, 451.

(18) See, for example: Stout, J. W.; Chisholm, R. C. *J. Chem. Phys.* **1962**, *36*, 979.

(19) Hatfield, W. E.; Weller, R. R.; Hall, J. W. *Inorg. Chem.* **1980**, *19*, 3285.

(20) Owen, J.; Harris, E. A. In "Electron Paramagnetic Resonance"; Geshwind, S., Ed.; Plenum Press: New York, 1972; p 427.

(21) Banci, L.; Bencini, A.; Gatteschi, D. *J. Am. Chem. Soc.* **1983**, *105*, 761.

(22) Kahn, O.; Charlot, M. F. *Nouv. J. Chim.* **1980**, *4*, 567.

(23) Yokota, M.; Koide, S. *J. Phys. Soc. Jpn.* **1954**, *9*, 953.

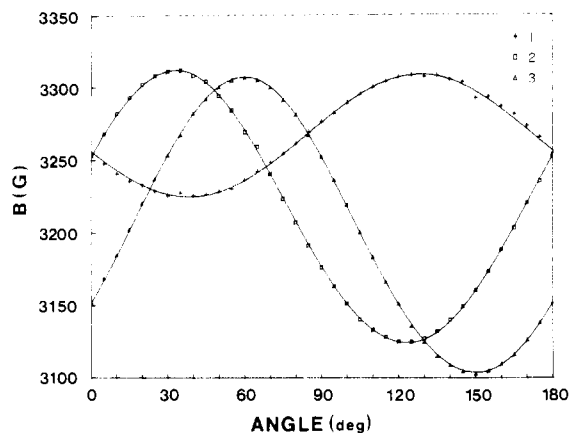


Figure 5. Plot of the angular dependence of the resonance field in the orthogonal system 1, 2, 3. The solid lines represent the best fits to eq 4.

or in terms of generalized Bloch equations.²⁶⁻²⁸ In the secular approximation both theories lead to the same result.²⁸ The latter approach gives a two-component EPR spectrum shape function $Y(B)$ as a first derivative of out-of-phase magnetization of the system (imaginary part of the total magnetization) in the weak microwave field.²⁸ Since only one line was observed in all rotations of the crystal, it was not possible to obtain information about interdimer exchange interactions.

Angular Dependence. Angular dependences of the resonance fields in the orthogonal system 1, 2, 3 show that the lines are merged completely. An angular g -factor dependence in the i th crystal rotation can be described by the general g^2 -tensor expression^{29,30}

$$g^2(i) = \alpha_i + \beta_i \cos 2\theta + \gamma_i \sin 2\theta \quad (3)$$

where θ is the azimuth angle of the magnetic field. The anisotropy parameters α , β , and γ can be calculated by a least-squares method from a set of equidistant (in angle θ) experimental points from the expressions³¹

$$\begin{aligned} \alpha_i &= n^{-1} \sum_{\theta=0}^M g^2(\theta) & \beta_i &= 2n^{-1} \sum_{j=0}^M g^2(\theta) \cos 2\theta \\ \gamma_i &= 2n^{-1} \sum_{\theta=0}^M g^2(\theta) \sin 2\theta \end{aligned} \quad (4)$$

where $n = 36$, $M = 175^\circ$ for data points collected in 5° intervals and $n = 18$, $M = 170^\circ$ for 10° intervals. The $B(\theta)$ plots with parameters calculated from eq 4 are presented by solid lines in Figure 5, where a good fit to the experimental points may be seen. A collection of α , β , and γ parameters for three orthogonal rotations enables the determination of the g^2 -tensor components. The following g factors were obtained from the rotational data in the manner described earlier by using the Waller-Rogers³² method:

$$g_z = 2.208 (1) \quad g_y = 2.055 (1) \quad g_x = 2.052 (1)$$

It is interesting to compare these g values to the molecular g values

Table IV. Bond Angles (deg) in the Cation $[\text{Cu}(\text{dien})\text{Br}]^+$

Br-Cu-Br'	89.37 (2)	N(1)-Cu-Br	95.9 (1)
N(1)-Cu-N(2)	84.0 (2)	N(2)-Cu-Br	178.8 (1)
N(2)-Cu-N(3)	86.4 (2)	N(3)-Cu-Br	94.1 (1)
N(1)-Cu-N(3)	160.6 (2)		
Cu-N(1)-C(1)	109.2 (3)	C(3)-N(2)-Cu	106.5 (3)
N(1)-C(1)-C(2)	109.2 (4)	N(2)-C(3)-C(4)	108.5 (4)
C(1)-C(2)-N(2)	105.6 (4)	C(3)-C(4)-N(3)	107.9 (4)
C(2)-N(2)-C(3)	116.3 (4)	C(4)-N(3)-Cu	107.4 (3)
C(2)-N(2)-Cu	108.0 (3)		

Table V. Bond Distances (Å) and Angles (deg) in the Perchlorate Ion

Cl-O(1)	1.38 (1)	Cl-O(3)	1.41 (1)
Cl-O(2)	1.40 (1)	Cl-O(4)	1.30 (1)
O(1)-Cl-O(2)	110.2 (3)	O(2)-Cl-O(3)	102.1 (4)
O(1)-Cl-O(3)	102.4 (4)	O(2)-Cl-O(4)	119.7 (4)
O(1)-Cl-O(4)	109.9 (4)	O(3)-Cl-O(4)	110.9 (6)

found earlier for $[\text{Cu}(\text{dien})\text{Cl}]_2(\text{ClO}_4)_2$. The chloro-analogue g values are³³

$$g_z = 2.214 (3) \quad g_y = 2.057 (3) \quad g_x = 2.048 (3)$$

Discussion

The magnetic exchange that occurs between metal ions in dimers can be explained as arising from direct metal-metal orbital overlap or by superexchange through the orbitals of the bridging ligand. In $[\text{Cu}_2(\text{dien})_2\text{Br}_2](\text{ClO}_4)_2$ the Cu-Cu distance of 3.790 Å rules out direct metal orbital overlap between the two coppers. Therefore, the exchange must be transmitted through the bromine bridging ligands.

There are many factors that influence superexchange. The nonbridging ligands have two important effects. First, these ligands affect the electron density at the metal atom, and second, through steric hindrance, they affect the geometry of the bridging unit. The symmetry of the bridging ligand orbitals and the electron density on the bridging ligand probably are the most important factors that affect superexchange. These effects arise largely through the nature of the overlap with metal orbitals. In some dimers the counterion may serve as an additional bridging ligand through which superexchange can occur. This has been seen in the complexes α - $[\text{Cu}(\text{dmaep})\text{OH}]_2(\text{ClO}_4)_2$,^{34,35} $[\text{Cu}(\text{bpy})\text{OH}]_2(\text{ClO}_4)_2$,^{4,36} and $[\text{Cu}(2\text{-miz})\text{OH}]_2(\text{ClO}_4)_2$,^{37,38} where exchange is transmitted through the hydroxo ligands as well as through the perchlorate ion. There is no evidence to suggest that the perchlorate ion is involved in intradimer coupling in $[\text{Cu}_2(\text{dien})_2\text{Br}_2](\text{ClO}_4)_2$.

Several geometrical parameters of the bridging unit are important. The most important of these include the metal-ligand bond lengths, R , the metal-ligand-metal bridging angle, ϕ , and the degree of planarity of the bridging unit, τ . Since these parameters determine which orbitals can interact and the extent to which they can overlap, there should be a direct correlation between the structure of a complex and its magnetic properties. It has been suggested^{10,39} that this magneto-structural correlation

- (24) Abragam, A. "The Theory of Nuclear Magnetism"; Oxford University Press: London, 1967; Chapters 4 and 10.
 (25) Lenk, R. "Brownian Motion and Spin Relaxation"; Elsevier: Amsterdam, 1977; Chapter 3.
 (26) Pople, A.; Schneider, W. G.; Bernstein, H. J. "High-Resolution Nuclear Magnetic Resonance"; McGraw-Hill: New York, 1959; Chapter 10.
 (27) Schotland, J.; Leigh, J. S. *J. Magn. Reson.* **1983**, *51*, 48.
 (28) Hoffmann, S. K. *Chem. Phys. Lett.* **1983**, *98*, 329.
 (29) Weil, J. A.; Buch, T.; Clapp, J. E. *Adv. Magn. Reson.* **1973**, *6*, 183.
 (30) Waller, W. G.; Rogers, M. T. *J. Magn. Reson.* **1975**, *18*, 39.
 (31) Hoffmann, S. K.; Corvan, P. J.; Singh, P.; Sethulekshmi, C. N.; Metzger, R. M.; Hatfield, W. E. *J. Am. Chem. Soc.* **1983**, *105*, 4608.
 (32) Waller, W. G.; Rogers, M. T. *J. Magn. Reson.* **1973**, *9*, 92.

- (33) Hoffmann, S. K.; Towle, D. K.; Hatfield, W. E.; Chaudhuri, P.; Wieghardt, K. *Inorg. Chem.* **1985**, *24*, 1307.
 (34) Lewis, D. L.; Hatfield, W. E.; Hodgson, D. J. *Inorg. Chem.* **1974**, *13*, 147.
 (35) McGregor, K. T.; Hodgson, D. J.; Hatfield, W. E. *Inorg. Chem.* **1976**, *15*, 421.
 (36) Haque, M.; Toofan, M.; Boshari, A. *Acta Crystallogr., Sect. A: Cryst. Phys., Diffraction, Theor. Gen. Crystallogr.* **1975**, *A31*, 583.
 (37) Reedijk, J.; Knetsch, D.; Nieuwenhuijs, B. *Inorg. Chim. Acta* **1971**, *5*, 568.
 (38) Ivarsson, G. J. M. *Acta Chem. Scand., Sect. A* **1979**, *33*, 323.
 (39) Fletcher, R.; Hansen, J. J.; Livermore, J.; Willett, R. D. *Inorg. Chem.* **1983**, *22*, 330.
 (40) Wilson, R. B.; Hatfield, W. E.; Hodgson, D. J. *Inorg. Chem.* **1976**, *15*, 1712.
 (41) Singh, Phirtu; Jeter, D. Y.; Hatfield, W. E.; Hodgson, D. J. *Inorg. Chem.* **1972**, *11*, 1657.
 (42) Jeter, D. Y.; Hatfield, W. E.; Hodgson, D. J. *Inorg. Chim. Acta* **1971**, *5*, 257.

Table VI. Structural and Magnetic Data for Bromo-Bridged Dimers

no.	compd ^a	ϕ , deg	R_0 , R , Å	Cu-Cu, Å	$2J$, cm ⁻¹	ϕ/R	ref
1	Cu ₂ (Maep) ₂ Br ₄	92.14	2.47, 2.80	3.80	-4.3	32.9	40
2	Cu ₂ (α -pic) ₂ Br ₄	100.4	2.43, 3.87	4.93	-5.0	25.9	41, 42
3	Cu ₂ (dmen) ₂ Br ₄	83.71	2.46, 2.87	3.57	-2.4	29.2	43, 44
4	Cu ₂ (dmg) ₂ Br ₄	85.59	2.39, 2.88	3.60	-3.6	29.7	45, 46
5	Cu ₂ (tmen) ₂ Br ₄	95.60	2.42, 3.20	4.20	-4.8	29.9	44, 47
6	Cu ₂ (4-metz) ₄ Br ₄	94.16	2.49, 3.03	4.063	-2.4	31.0	48
7	[Cu(dien)Br] ₂ (ClO ₄) ₂	89.37	2.42, 2.89	3.79	+2.7	30.96	b

^a Abbreviations: Maep = 2-(2-methylaminoethyl)pyridine; α -pic = α -picoline; dmen = *N,N*-dimethylethylenediamine; dmg = dimethylglyoxime; tmen = *N,N,N',N'*-tetramethylethylenediamine; dien = diethylenetriamine; 4-metz = 4-methylthiazole. ^b This paper.

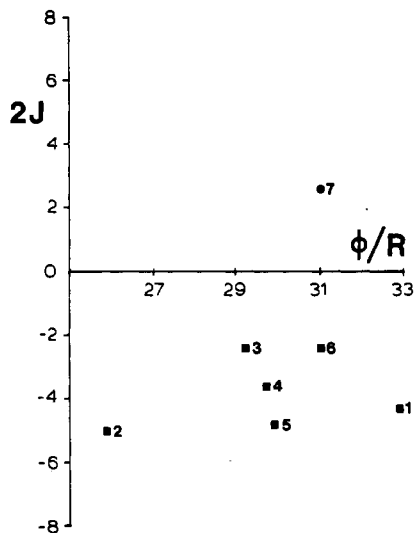


Figure 6. $2J$ and ϕ/R data for bis(μ -bromo)-bridged Cu(II) dimers. The data are numbered as in Table VI. The filled circle represents the data for [Cu₂(dien)₂Br₂](ClO₄)₂.

should consist of a family of curves (a surface) that results from plotting $2J$ vs. R , ϕ , τ , and other structural parameters.

Magneto-structural correlations have been found for bis(μ -hydroxo)-⁴⁻⁶ and bis(μ -chloro)-bridged Cu(II) dimers.⁸⁻¹⁰ All of the data for the bis(μ -hydroxo)-bridged dimers fall on a straight

line when $2J$ is plotted against the value of the copper-oxygen-copper bridging angle, ϕ . The addition of another structural parameter, the copper-chlorine long bond distance R , was needed for the bis(μ -chloro)-bridged dimer correlation. In the case of the chloro complexes, the data fall on a smooth curve when $2J$ is plotted against ϕ/R .

The data for all known bis(μ -bromo)-bridged copper(II) dimers that have been both magnetically and structurally characterized are given in Table IV. The single-triplet splitting is small in all of the complexes, and the singlet state is the ground state for all but [Cu(dien)Br]₂(ClO₄)₂. The shorter copper-bromine bond distances of the Cu₂Br₂ units vary little from each other, but the longer distances vary from 2.80 to 3.87 Å. The $2J$ and ϕ/R data for the bromo complexes are shown in Figure 6. The data clearly do not lie on a smooth curve. Plots of $2J$ vs. ϕ and $2J$ vs. the copper-copper distance do not yield smooth correlations.

It is interesting to note that although the value of ϕ/R for [Cu(4-metz)₂Br₂](ClO₄)₂ (31.0) is similar to that for [Cu₂(dien)₂Br₂](ClO₄)₂ (30.96), the values of $2J$ for the complexes are very different (-2.4 vs. +2.7). It is clear that there is no "simple" magneto-structural correlation for bis(μ -bromo)-bridged copper(II) dimers as has been found for bis(μ -hydroxo)- and bis(μ -chloro)-bridged copper(II) complexes. Continued research should reveal what additional factors are important in determining the sign and magnitude of ΔE_{ST} . Also, it may be that the ΔE_{ST} value deduced from the magnetic data for [Cu₂(dien)₂Br₂](ClO₄)₂ reflects interdimer exchange that is evident from the magnetic data at low temperature.

Acknowledgment. This research was supported by the National Science Foundation (Grant No. CHE 83 08129).

Registry No. [Cu(dien)Br]₂(ClO₄)₂, 99232-61-8.

Supplementary Material Available: Listings of thermal parameters, calculated positions of hydrogen atoms, and observed and calculated structure factors (14 pages). Ordering information is given on any current masthead page.

- (43) Phelps, D. W.; Goodman, W. H.; Hodgson, D. J. *Inorg. Chem.* **1976**, *15*, 2266.
 (44) Estes, W. E. Ph.D. Dissertation, The University of North Carolina at Chapel Hill, 1977.
 (45) Megnamisi-Belombe, M.; Novotny, M. A. *Inorg. Chem.* **1980**, *19*, 2470.
 (46) Endres, H. *Acta Crystallogr., Sect. B: Struct. Crystallogr. Cryst. Chem.* **1978**, *B34*, 3736.
 (47) Luukkonen, E.; Pajunen, A. *Suom. Kemistil. B* **1973**, *22*, 330.
 (48) Marsh, W. E.; Bowman, T. L.; Harris, C. S.; Hatfield, W. E.; Hodgson, D. J. *Inorg. Chem.* **1981**, *20*, 3864.